JOURNAL OF AIRCRAFT
Vol. 31, No. 1, Jan.–Feb. 1994

Variable-Complexity Aerodynamic Optimization of a High-Speed Civil Transport Wing

M. G. Hutchison,* E. R. Unger,† W. H. Mason,‡ B. Grossman,§ and R. T. Haftka¶
Virginia Polytechnic Institute and State University, Blacksburg, Virginia 24061

A new approach for combining conceptual and preliminary design techniques for wing optimization is presented for the high-speed civil transport (HSCT). A wing-shape parametrization procedure is developed which allows the linking of planform and airfoil design variables. Variable-complexity design strategies are used to combine conceptual and preliminary-design approaches, both to preserve interdisciplinary design influences and to reduce computational expense. In the study, conceptual-design-level algebraic equations are used to estimate aircraft weight, supersonic wave drag, friction drag, and drag due to lift. The drag due to lift and wave drag are also evaluated using more detailed, preliminary-design-level techniques. The methodology is applied to the minimization of the gross weight of an HSCT that flies at Mach 3 with a range of 6500 mi.

Introduction

THE design of an advanced aircraft requires the prediction of the system response and performance in three distinct phases: 1) conceptual, 2) preliminary, and 3) detailed design. As the aircraft design progresses through these stages the analysis methodology becomes increasingly sophisticated. Typically, the conceptual design of the system is performed using simple experienced-based algebraic expressions (often in the form of statistical analyses), based on experience and on elementary models of the system. These expressions are implemented in conceptual design sizing programs such as FLOPS[1] or ACSYNT.[2] In the preliminary design phase, system performance is predicted by more complex numerical simulations such as aerodynamic panel methods or structural plate model approximations. Computational constraints often dictate that the models used at this stage are basic and may not include all the complicating factors such as nonlinearities. Finally, at the detailed design level, the full force of state-of-the-art computation is brought to bear for all analyses.

In the second and third design stages, the multidisciplinary aspects of the system are often expressly neglected. At the conceptual level, the tradeoffs between the requirements of different disciplines are easily addressed due to the simplicity of the modeling of the system. However, as soon as detailed numerical simulations begin, it is very difficult to preserve interdisciplinary communications, partly because of computational cost, and partly because of the compartmentalization of expertise.

The principal goal of multidisciplinary design optimization is to address this lack of communication at the higher design levels in order to design better aircraft. Unfortunately, direct integrated design remains prohibitively expensive computationally for two reasons. First, intuitive shortcuts that are available in single-discipline design are not applicable for multidisciplinary design. Second, integrated design requires the costly calculation of interdisciplinary sensitivities, such as the derivatives of aerodynamic performance with respect to changes in aircraft structural components. Previous work by our group at Virginia Tech in the area of multidisciplinary design, has centered on the development of more efficient computational methods for evaluating the interdisciplinary sensitivities and on the implementation of sequential approximate optimization techniques.[3,4] Related work in other areas of multidisciplinary optimization is presented in Refs. 5–8.

In this article we demonstrate a variable-complexity modeling approach[9] to the design of a high-speed civil transport (HSCT) wing. We design the wing to minimize takeoff gross weight of a Mach 3 configuration with a range of 6500 mi. We have investigated two aspects of this technique. First, we address the difficulty of retaining cross-disciplinary influences by coupling a detailed analysis model for one discipline with a simple model for another. Specifically, we show results for preliminary aerodynamic design which includes structural considerations through the use of a conceptual design (algebraic) structures model. Secondly, we show that the computational expense associated with repetitive calculations in a numerical optimization may be significantly reduced by combining a preliminary-design-level analyses with simpler conceptual-design-level models. In the context of the wing designs, we employed two levels of modeling in the evaluation of both aircraft wave drag and drag due to lift.

We use the NASA AST3I concept[10] as a baseline for the design optimization. This concept was developed at the Langley Research Center and reflects the best aspects of current advanced configuration design practice. The aircraft is a Mach 3, 6500-mi. range design with details of the geometry and weights described by Robins et al.[10] In addition, a wind-tunnel model of the AST3I was tested,[11] establishing a basis for evaluating aerodynamic estimation methods.

Previous interdisciplinary wing design studies have concentrated on planform design with given airfoils. In the present work we venture into simultaneous design of the planform and the airfoil. To keep the number of design variables manageable, we utilize features of the AST3I design to define the connection between the planform and airfoil variables.

In the following sections, we describe the method used to define the wing shape for optimization, define the design problem, outline the methods utilized, and describe the op-

Presented as Paper 92-0212 at the AIAA 30th Aerospace Sciences Meeting and Exhibit, Reno, NV, Jan. 6–9, 1992; received Feb. 24, 1992; revision received Oct. 27, 1992; accepted for publication Nov. 2, 1992.

*Graduate Assistant, Department of Aerospace and Ocean Engineering; currently Engineer, Aurora Flight Sciences Corporation, Manassas, VA.

†Graduate Assistant, Department of Aerospace and Ocean Engineering; currently NRC Fellow, NASA Langley Research Center.

‡Associate Professor, Department of Aerospace and Ocean Engineering. Associate Fellow AIAA.

§Professor and Head, Department of Aerospace and Ocean Engineering. Associate Fellow AIAA.

¶Christopher C. Kraft Professor, Department of Aerospace and Ocean Engineering. Associate Fellow AIAA.

timization method and strategy. Finally, optimization results and our conclusions are presented.

Wing Shape Representation

Successful optimization requires a simple, yet meaningful characterization of the geometry to be optimized. Our analytic wing definition provides a general, yet practical geometry using a small number of design variables. The wing is defined in terms of planform and airfoil thickness definitions. The airfoil sections are related to the planform based on current aerodynamic design practice. The actual cambering of the wing, once the thickness distribution and planform have been determined, should only have a minor effect on the wing weight. Therefore, for the aerodynamic design of the wing, we emphasize the planform and the thickness distribution and assume that the wing can be cambered as required.

We distinguish between the parametric model and the numerical description of the wing. As described below, the parametric model utilizes a small set of design variables to define the wing shape, but the aircraft geometry is actually described numerically in the Craidon geometry format.[12] This approach allows the use of analysis methods that utilize this discrete description directly. In this article, we address only the design of the aircraft wing, and use the fuselage, fin, and nacelles directly from the AST3I geometry description.

Planform Description

The planform is specified by defining the leading and trailing edges using a blending of linear segments. The exponential blending was apparently first used by Barnwell,[13] and was later employed in the development of the SC3 wing concept.[14] The leading- and trailing-edge equations are defined by the projected intersection points (i.e., the planform break points), the axial location of the wing tip, the wing semispan, and the wing-tip chord.

Exponential blending is used to provide a smooth transition between the straight-line segments. The blending is controlled by a parameter Δ_i, determined by the degree of blending desired, with large values corresponding to increased blending. For the cases presented, the values of Δ_i were not varied. The details of the equation definitions are given in Ref. 15. For this work, we utilized three blended linear segments for both the leading and trailing edges with the wing planform described by 11 variables, $x_1 \rightarrow x_{11}$, as illustrated in Fig. 1. As we utilize the fuselage from the baseline configuration, the locations of the leading and trailing edges at the root are fixed. Reference 15 showed that the difference between the parametric description of the AST3I and the data is minimal.

Airfoil Description

Using the AST3I as a basis, airfoils with both sharp and round leading edges are used in the definition of the wing. Although the AST3I concept uses 6A-series airfoils, the requirement for simplicity led to the use of airfoil definitions based on (but not the same as) the classical NACA 4-digit modified airfoil definition. Specifically, the thickness distribution for the round-nosed airfoils has been modified to reduce the curvature on the aft portion of the airfoil in comparison to the usual NACA 4-digit and modified 4-digit airfoils (bringing it into much closer agreement with the 6A series).

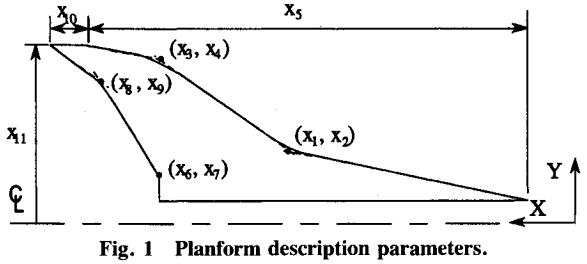

Fig. 1 Planform description parameters.

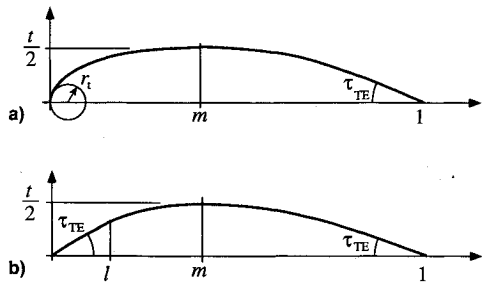

Fig. 2 Airfoil definition parameters: a) round leading edge and b) sharp leading edge.

For sharp-nosed airfoils a straight-line segment is defined at the leading edge. The complete details are given in Ref. 15. The five parameters required to define an airfoil thickness distribution are the leading-edge radius size parameter I [as in the NACA modified 4-digit airfoil definition, the leading-edge radius to chord ratio r_t is defined by $r_t = 1.1019(tI/6c)^2$]; or the leading-edge half-angle τ_{LE}; the trailing-edge half-angle τ_{TE}; the thickness-to-chord ratio t/c; the chordwise location of the end of the linear segment on sharp-nosed airfoils l; and the location of the maximum thickness m (Fig. 2). In practice, we found that a fixed value of $l = 5\%$ of chord worked well over a broad range of airfoils. With these models, the errors in the airfoil representation were under 2%, compared to AST3I data.

Planform/Airfoil Integration

To limit the number of design variables, the airfoil used at a particular spanwise station is related to the planform at that station by a set of rules based on the design of the baseline configuration. Thus, in this article, the wing geometry is defined by the following:

1) The wing t/c is specified at four control stations on the wing semispan, and the thickness, not t/c, is varied linearly between these control points.

2) The chordwise location of maximum thickness m is constant across the span.

3) The airfoil shape is sharp or round locally, depending upon whether the local leading edge is supersonic or subsonic.

4) The leading-edge half-angle τ_{LE} varies linearly with the thickness-to-chord ratio.

5) The leading-edge radius size parameter is a constant for all round leading edges.

6) The trailing-edge half-angle τ_{TE} varies linearly with the thickness-to-chord ratio.

Design Problem

The design problem is the optimization of an HSCT wing to minimize takeoff gross weight for a specified range, payload, and cruise Mach number. For this work, we have considered a Mach 3 vehicle with a range of 6500 mi. The choice of gross weight as the figure of merit (objective function) directly incorporates both aerodynamic and structural considerations, in that the wing structural weight directly affects aircraft empty weight, while aerodynamic performance dictates the required mission fuel. The optimization is performed with a fixed fuselage and nacelle geometry.

The engine size and specific fuel consumption were fixed in the design optimization at 50,000-lb maximum sea-level static thrust per engine, and cruise specific fuel consumption constant at 1.3 lb/(lb·h). This simple approach is based on the consideration that the engine size is determined by the takeoff requirement.[16] A more sophisticated propulsion model could be included in the analysis without a fundamental change in the approach.

Design Variables

Table 1 shows the 21 design variables used to describe the wing and flight mission. They fall into three categories: 1) wing planform, 2) airfoil, and 3) mission definition variables.

The 11 planform design variables are based directly on the blended linear equation approach described earlier. As may be seen in Table 1 and Fig. 1, we define the (x, y) location of the leading and trailing-edge break points, the axial location of the wing tip, the wing semispan and the tip chord. The root locations of the leading and trailing edges are fixed by the baseline configuration.

The seven airfoil thickness definition variables are used to quantify the previously described rules linking the airfoil to the wing planform. The constants in these definitions were chosen based on the AST3I geometry.

Finally, we utilize three variables to define an idealized cruise mission. We do not take account of takeoff and climb to altitude, and the aircraft is assumed to begin cruise at its gross weight. The aircraft range is determined by the distance flown in cruise that consumes 85% of the mission fuel. The remaining 15% is assumed to be reserve fuel, a value based on the AST3I configuration. We use two design variables to define the initial cruise altitude and a constant climb rate. The latter allows the optimizer to define an approximate cruise-climb followed by constant altitude flight at the specified altitude limit.

Constraints

As summarized in Table 2, we employ 37 constraints which may be divided into two categories: 1) geometric and 2) performance constraints. The geometric constraints prevent physically unrealistic or impossible designs. Specifically, the wing chords at all locations were required to be greater than 7 ft, the width of the wing normal to the leading edge was required to be greater than 3 ft, and the wing t/c ratios were not allowed to be less than 1.5% at the four wing thickness definition locations. The wing break point locations were forced to be arranged sequentially on the wing and to be less than the wing semispan. In an effort to prevent unrealistic geometries, we required that the sweep angle of the trailing edge be positive (i.e., rearward sweep). In one of the designs presented in Ref. 15, we examined the effect of relaxing this constraint during the design process.

The performance constraints include a required range of at least 6500 mi. To prevent tail-scrape, the landing angle of attack was not allowed to exceed 12 deg. We assumed that the mission fuel for the aircraft was carried entirely in the wing and required that 50% of the wing volume was sufficient for storing the fuel. The lift coefficient at an emergency landing (145 kt at 5000 ft with 50% fuel load on a 90°F day) was required to be no more than 1. The section lift coefficients at the same conditions, assuming an elliptic lift distribution, were not allowed to exceed 2. Finally, the altitude is limited to 70,000 ft for cabin depressurization safety considerations. This constraint is enforced by keeping the altitude constant once the aircraft has reached this altitude, so that it does not appear as an explicit constraint in the optimization procedure.

Table 1 Design variables

(11) Planform	(7) Airfoil	(3) Performance
x At LE breaks 1, 2	t/c At root	Flight fuel
y At LE breaks 1, 2	LE Breaks 1, 2 and tip	Climb rate
x At TE breaks 1, 2	max t/c Location	Initial cruise altitude
y At TE breaks 1, 2	LE Radius and half-angle	
x Of LE wing tip		
Tip chord		
Wing semispan		

Table 2 Design constraints

(21) Geometric	(16) Performance
Eleven wing chords	Range
Four wing thicknesses	Landing α
Four break points	Fuel volume
Wing minimum width	Landing C_L
Root trailing-edge angle	Landing section C_l
	Maximum altitude

Analysis Methodology

The analysis techniques utilized include a conceptual-level model for the structural influence on the aircraft weight, several models and levels of approximation for the aerodynamic drag, calculation of the aircraft range, and the estimation of landing angle of attack.

Structures

To include the influence of structural considerations on the wing design, we have adopted the weight equations developed by McCullers.[1] These are traditional weight-estimating relations consistent with modern conceptual-level aircraft sizing programs. These equations enable us to incorporate weight penalties for wing designs that are more structurally demanding. Details of the wing-weight equation and the calculation of aircraft gross weight are presented in Ref. 15.

We note here that the original version[15] of this article contained results which utilized an erroneous weight estimation program. The weight estimation equations in Ref. 15, equations B.1–B.13, were programmed incorrectly. The design results and conclusions in this article reflect the corrected program.

Aerodynamics

The key analysis is the calculation of drag, consisting of the contributions from volumetric wave drag, drag due to lift, and friction drag. In keeping with the philosophy of variable-complexity modeling, we have used detailed and approximate models for both the wave drag and the drag-due-to-lift calculations. The approximate models, methods typically used in the conceptual design phase, are algebraic or require simple quadrature integrations. The detailed models utilized more exact methods requiring computer codes and represent the types of analyses required at the preliminary design stage. We describe the implementation of the different models in the optimization process later.

Volumetric Wave Drag: Detailed Model

Wave-drag estimates are calculated using the classic Harris wave-drag program.[17] This program computes the value of the far-field integral arising from slender-body theory, and has been found to adequately predict the wave drag of supersonic transport class aircraft.

Volumetric Wave Drag: Algebraic Model

An approximate estimation of wave drag is obtained using a semiempirical algebraic model developed in Ref. 18 for trapezoidal planforms. The approximate model depends on wing t/c ratio; the chordwise location of maximum airfoil thickness m; the airfoil leading-edge radius to chord ratio r_t; wing leading and trailing-edge sweep angles Λ_{LE} and Λ_{TE}, respectively; the wing taper ratio λ; the wing aspect ratio; and the flight Mach number.

To use the approximate model, a trapezoidal wing that is approximately equivalent in terms of wave drag to the actual wing is needed. This wing will be referred to as the equivalent wave-drag wing. The t/c ratio is obtained by averaging the values in the numerical description of the wing, the parameter m is defined directly in the design variables, and the subsonic value of leading-edge radius (also a design variable) is used to define r_t. We use a wing taper ratio of $\lambda = 0.1$ for all the data presented. This value was found to produce good results over a broad range of wing designs. The leading-edge sweep

angle is defined using a weighted-average value determined from the discrete numerical description of the actual wing. The trailing-edge sweep angle is defined from the trapezoidal wing geometry.

The wave drag of this equivalent wing is calculated using the relations in Ref. 18. An estimate of the contributions due to the remainder of the aircraft, obtained using the Harris code, is subsequently added. This contribution is held constant for a given flight Mach number, and the approximate model analysis, for any wing design, is therefore independent of the detailed analysis.

Figure 3 compares the wave drag estimated by the two methods for a number of different wing designs. Using the parametric model, a wing geometry is defined using a vector of design variables $\boldsymbol{x}$. The wave drag data was calculated at different values of $\boldsymbol{x}$, varied between two points $\boldsymbol{x}_0$ and $\boldsymbol{x}_1$ in the design space (described in a later section, $\boldsymbol{x}_0$ and $\boldsymbol{x}_1$ define the initial and final designs, respectively), as a function of the relative design-change parameter ξ in the expression

$$\boldsymbol{x} = \boldsymbol{x}_0 + \xi(\boldsymbol{x}_1 - \boldsymbol{x}_0) \tag{1}$$

where $0 \leq \xi \leq 1$.

The algebraic model wave drag is within 6% of the Harris wave drag, and it displays similar trends over a range of wing designs. Note that the Harris code results are not smooth. While of little concern in the estimation of the drag, this behavior makes the calculation of derivatives of the wave drag with respect to design variables inaccurate. By contrast, the algebraic model produced very smooth results that allow for consistent derivative evaluation. These features are of particular importance in our later discussion of drag approximations used in the optimization problem. Computationally, the time required to calculate the drag using the algebraic model is more than two orders of magnitude smaller than that required for the Harris model.

Drag Due to Lift: Detailed Model

The estimation of drag due to lift from linear theory may be reduced to the calculation of the drag polar shape parameter $1/C_{L_\alpha} - C_T/C_L^2$, where C_{L_α} is the wing lift-curve slope, and C_T is the thrust coefficient. The component of drag due to lift is then given by

$$C_{D_l} = (1/C_{L_\alpha} - C_T/C_L^2)C_L^2 \tag{2}$$

For this analysis, we adopt the methods developed by Carlson et al.[19,20] which use the integral solution to the linearized supersonic potential equation for wings of arbitrary planform.

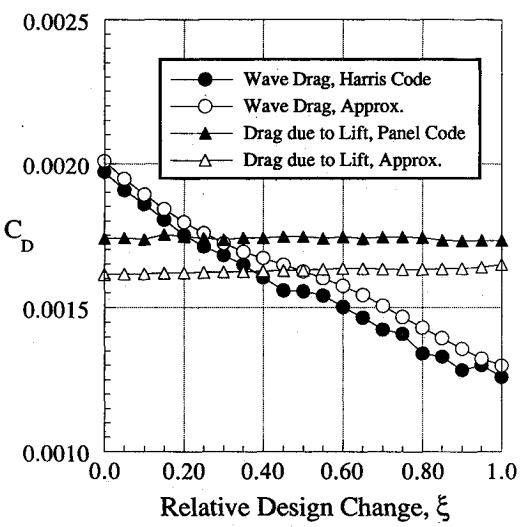

Fig. 3 Algebraic and detailed drag calculations.

The panel method implementation provides a prediction of the drag due to lift. The value of C_T obtained from linear theory can be reduced to levels found experimentally using Carlson's "attainable thrust" concept.[20]

Drag Due to Lift: Algebraic Model

To approximate the drag due to lift, the wing is replaced by an equivalent arrow wing. Assuming that the flow can be described by linearized supersonic thin-wing theory, algebraic analytic solutions are available for arrow wings.[21] The first step is to define a correspondence between a general wing planform and an arrow wing.

The aerodynamic characteristics of an arrow wing are determined by two geometric parameters: 1) the leading- and 2) trailing-edge sweep angles. Using a discrete numerical description of an arbitrary planform, we defined an aerodynamically equivalent arrow wing. The leading-edge sweep is defined using the root value of the planform sweep. The trailing-edge angle is defined using a weighted-average sweep value over the trailing-edge data points.

Drag due to lift reductions achieved through camber and twist are simulated by reducing the zero leading-edge suction (LES) polar, C_L^2/C_{L_α}, by a fraction of the full value of leading-edge suction, C_T, predicted by linear theory. The fraction of C_T included is chosen using Carlson's experimentally based estimates for the percentage of LES achievable.

Figure 3 also shows the drag due to lift (at $C_L = 0.05$) over a range of wing designs. The panel code also produces unsmooth results presenting difficulties in the evaluation of drag-due-to-lift derivatives. In contrast, the algebraic model yields smooth results. Computationally, the time required to calculate the drag using the algebraic model is more than two orders of magnitude smaller than that required for the panel code.

Friction Drag

Skin friction is computed using standard algebraic estimates. The boundary layer is assumed to be turbulent. The van Driest II method, as discussed by Hopkins and Inouye,[22] has been utilized and form-factor corrections have been applied to account for the effect of surface curvature.

The accuracy of the methods employed was assessed in Ref. 15, where the drag polar computed using the detailed methods described above was compared to the AST3I wind-tunnel data. The aircraft geometry used in the calculation was the initial set of design variables, selected to match the AST3I geometry. The result showed that the detailed models provide a good estimate of the aerodynamic performance for this class of configurations, and that the design variables are adequate to represent the AST3I geometry.

Range Calculation

The aircraft range is calculated at a constant cruise Mach number of 3 until the available fuel is exhausted. As described earlier, we assume that 85% of the mission fuel is used in cruise, with the remaining 15% held as reserve. The range is determined by a time integration of the velocity. The amount of fuel spent is found from a time integration of the product of the specific fuel consumption and the drag during cruise. The first portion of the cruise is a cruise-climb profile with the initial altitude and climb rate determined from the design variables. The latter portion of the cruise begins when the aircraft reaches its maximum allowable altitude, at which time the altitude is held constant at this value.

Landing Angle of Attack

For the low-aspect ratio configurations in this class, the angle of attack at landing must be limited to avoid problems with tail-scrape. To find the attainable lift coefficient at the prescribed landing angle, potential-flow lift, nonlinear vortex

lift, and ground effects were considered. We employ a variable-complexity strategy whereby a vortex lattice method is coupled to a simple algebraic model[23] to estimate the lift as a function of angle of attack.

Initial designs[15] used only an approximate algebraic model for the landing angle-of-attack calculation. Corrections to the wing-weight calculation (discussed earlier) produced designs which were more sensitive to the landing angle-of-attack model. This necessitated using the variable-complexity strategy.[24]

Optimization Procedure and Strategy

The numerical optimization is performed using the NEWSUMT-A program[25] which employs a sequential unconstrained minimization technique utilizing an extended interior penalty function. Newton's method with approximate second derivatives is used for unconstrained minimization.

The primary computational cost of the optimization is not the evaluation of the objective function, but rather the estimation of the drag components used in the range calculation. Because derivatives of the constraints are evaluated by finite differences, the optimizer requires many hundreds of constraint evaluations to complete the optimization, and thus the direct use of the Harris program for wave drag and the supersonic panel method for drag due to lift in the range calculation is prohibitively expensive. To reduce this expense, a sequential approximate-optimization technique was employed in which the overall design process is composed of a sequence of optimization cycles. At the beginning of each cycle, approximations to the wave drag and drag due to lift are constructed and move limits imposed on the design variables to avoid large errors.

In the following, we describe several approaches to the approximation of the wave drag and the drag due to lift. To generalize the discussion, we consider approximations to a scalar function f that depends on the vector of design variables $\boldsymbol{x}$. In the context of the estimation of wave drag, f is C_{D_w}, the wave drag coefficient. For drag due to lift, f is the parameter $1/C_{L_\alpha} - C_T/C_L^2$. We utilize the detailed and the algebraic models for these components of drag, described earlier, and refer to the results from these models as f_d and f_a, respectively. We consider linear, global-local, and scaled approximations.

Linear Approximation

The linear approximation is simply a first-order Taylor series expansion in the design variables about the design point at the beginning of a cycle, $\boldsymbol{x}_0$, using the detailed analyses

$$f(\boldsymbol{x}) \approx f_d(\boldsymbol{x}_0) + \nabla f_d \Delta \boldsymbol{x} \tag{3}$$

where $\Delta \boldsymbol{x} = \boldsymbol{x} - \boldsymbol{x}_0$ and ∇f_d is evaluated at $\boldsymbol{x}_0$. The gradient of f_d is a row vector composed of elements $\partial f_d/\partial x_i$. These partial derivatives are estimated by forward differences. For smooth functions, the stepsize Δx_i is chosen small enough to obtain an adequate representation of the derivative without incurring roundoff error. For noisy functions, small values of Δx_i produce large errors in the derivatives. To reduce this problem, we employ $\Delta x_i = 0.01 x_i$ in order to make Δx_i larger than the scale of some of the noise.

Global-Local Approximation (GLA)

This approximation technique,[26] utilizes an approximate model in conjunction with a more detailed analysis. In the context of this article, the detailed analyses are the Harris code and the panel code, and the approximate models are the algebraic models described previously. The approximation utilizes a linear scaling technique, whereby f is evaluated at $\boldsymbol{x}$ using

$$f(\boldsymbol{x}) \approx \beta(\boldsymbol{x}) f_a(\boldsymbol{x}) \tag{4}$$

where the scaling parameter is evaluated at the design point at the beginning of a cycle $\boldsymbol{x}_0$ as

$$\beta(\boldsymbol{x}_0) = \frac{f_d(\boldsymbol{x}_0)}{f_a(\boldsymbol{x}_0)} \tag{5}$$

The scaling parameter is approximated at $\boldsymbol{x}$ using a Taylor series expansion

$$\beta(\boldsymbol{x}) \approx \beta(\boldsymbol{x}_0) + \nabla \beta \Delta \boldsymbol{x} \tag{6}$$

The gradient of β at $\boldsymbol{x}_0$ involves differentiating (5), and requires the evaluation of the gradients of both the detailed and algebraic analyses. As for the linear approximation, we utilized forward finite differences with $\Delta x_i = 0.01 x_i$. The unreliable derivative estimates (from both the Harris program and the panel code) can cause large errors in both the linear and GLA approximations. These errors mandate the use of small move limits in the design variables, and can increase the number of cycles required for a complete optimization.

Scaled Approximation

As indicated in Fig. 3, the approximate, algebraic models produce trends similar to the detailed analyses, even if the actual magnitudes of the results differ. Such models suggest the use of a constant scaling function for an approximation

$$f(\boldsymbol{x}) \approx \beta(\boldsymbol{x}_0) f_a(\boldsymbol{x}) \tag{7}$$

where β is given by Eq. (5).

Two related features of this approach make it particularly appealing: 1) it eliminates the dependence of the approximation function f on derivatives of the detailed analysis, and 2) as a result, the CPU time required to set up the approximation at the beginning of each cycle is dramatically reduced.

Figure 4 shows the wave drag coefficients calculated for an aircraft with a wing described by a design vector $\boldsymbol{x}$, given by Eq. (1). Designs $\boldsymbol{x}_0$ and $\boldsymbol{x}_1$ are at the beginning and end of optimization cycle eight within the context of the sequential optimization procedure, and differ from each other by less than 7%. In the figure, the wave drag calculated using the detailed wave-drag model (i.e., the Harris program) is compared with the results given by the three approximation methods described above. The difficulties caused by the oscillations in the detailed model calculations for the derivative-based linear and GLA approximations are apparent.

Although the drag errors appear relatively small, the range of this class of aircraft is so sensitive to changes in the drag that the differences between the approximate calculations and the detailed model results at the end of a design cycle present

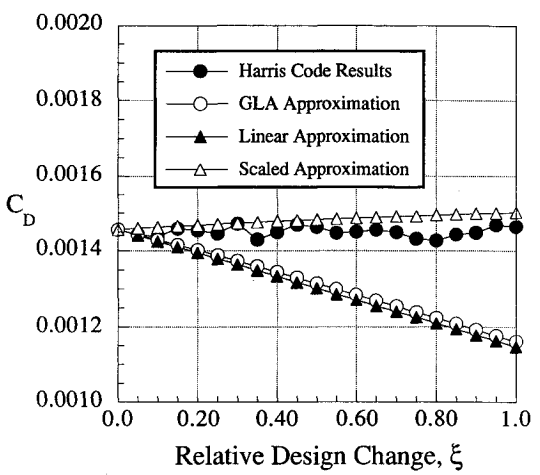

Fig. 4 Wave drag approximations.

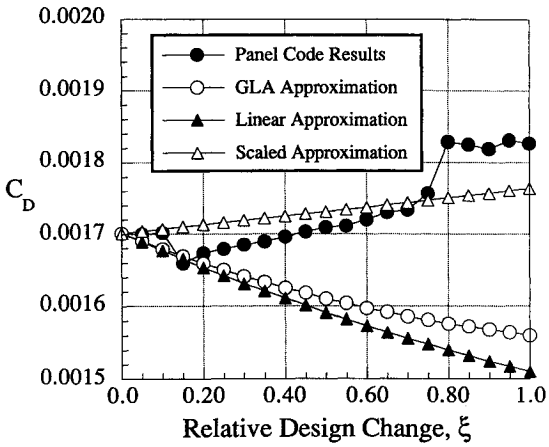

Fig. 5 Drag due to lift approximations.

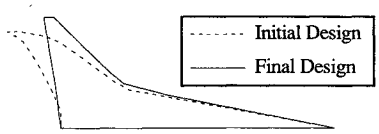

Fig. 6 Initial and final planforms.

significant difficulties in the optimization procedure. Since the drag calculated at the beginning of a design cycle is given by the detailed model results for all three approximation methods, the range at the end of a design cycle is usually not equal to the range at the beginning of the next cycle.

Figure 5 shows the variation of drag-due-to-lift coefficients with the same relative design change as described in connection with Fig. 4. The drag values shown were calculated using $C_L = 0.05$. The detailed model results, as well as the three approximate methods, are shown. In both Figs. 4 and 5 the scaled approximation is better than the linear and the GLA approximations because of errors in the calculation of the derivatives. This is not always the case; in some design cycles, the linear or GLA approximation is more accurate.

Results

The initial and final planforms for the optimization are shown in Fig. 6. The initial design represents an evaluation of the parametric model of the AST3I using the methods described above. The optimization problem converged in 42 cycles with the move limits gradually reduced from an initial value of 7% to a final value of 1%. Only three constraints were active at the conclusion of the optimization: 1) the landing angle-of-attack limitation, 2) the range constraint, and 3) the altitude limitation.

Table 3 presents some details of the initial and final designs. (The initial design differs from that used in Ref. 15 reflecting weight parameters more consistent with Ref. 10.) The final design weighs less than the initial design, and meets the range and landing angle-of-attack requirements. The principal design changes were to decrease the inboard leading-edge sweep and the outboard sweep and reduce the wing thickness. The wing area increased only 3.8%, but the span increased by 13.8% for an increase of 24.7% in the aspect ratio. The tendency in the design was to trade increased wing weight (thinner wings) for aerodynamic efficiency (decreased wave drag) to save mission fuel. As may be seen in Table 3, the wing weight increased while fuel weight decreased for a net savings.

Aerodynamically, the final configuration shows improvement in wave drag and drag due to lift (see Table 3). There was an increase of 13.8% in the maximum L/D ratio from the initial to final design. While the aircraft flies close to the maximum L/D ratio (initial cruise: $L/D = 8.68$, final cruise: $L/D = 8.51$), the altitude limitation restricts the ability to fly a more nearly optimal cruise profile.

Table 3 Initial and final designs

	Initial design	Optimum design
Weights, lb × 10^5		
Gross weight	6.609	6.153
Wing weight	0.735	0.819
Fuel weight	3.400	2.872
Range margin, %	−0.45	0.26
Landing angle margin, %	−19.8	0.58
Sweep, deg		
Inboard LE	79.56	78.80
Outboard LE	53.13	49.82
Inboard TE	0.00	7.65
Outboard TE	27.14	11.40
Thickness, % t/c		
Root	2.000	2.079
LE Break 1	3.500	1.918
LE Break 2	3.500	1.614
Tip	3.500	1.513
Drag, lb × 10^3, at start of cruise		
Wave drag	17.19	14.08
Friction drag	31.08	33.34
Drag due to lift	34.85	23.45
L/D max	8.050	9.162
Wing weight/area, lb/ft^2	5.950	6.384
Wing area, ft^2 × 10^4	1.236	1.283
Aspect ratio	1.835	2.288

Conclusions

We have demonstrated a variable-complexity modeling approach to the design of an HSCT wing. The difficulty of retaining cross-disciplinary influences was addressed by coupling relatively detailed aerodynamic models with a conceptual-design structural model. Computational costs were reduced by coupling detailed aerodynamic models with simple algebraic models in the optimization process. A very efficient parametrization of HSCT class wing planforms and thickness distributions was developed. Utilizing only 18 design geometric design variables, we were able to obtain designs with significantly decreased gross weight at a specified range and payload, while satisfying performance and geometric constraints. However, due to some differences in mission, modeling, and constraints, (e.g., we did not consider trim, stability considerations, and sonic boom), these improvements should not be construed as indications of deficiencies in the AST3I design.

We have identified the problem that the drag components obtained from the detailed aerodynamic models were noisy and resulted in poor derivatives. This led to convergence oscillations and range errors, and highlights the need for approximation methods that do not depend on refined model derivatives. Nevertheless, the variable-complexity approach to drag modeling proved adequate to converge the design and allowed the optimization to proceed without excessive computational expense.

Acknowledgments

This work was supported by NASA Langley Research Center under Grant NAG-1-1160 and the National Science Foundation under Grant DDM-9008451. This support is gratefully acknowledged. The authors would like to thank L. A. McCullers of ViGYAN Research Associates for his help in implementing the weight relations from FLOPS and P. Coen of NASA Langley for providing us with wind-tunnel data on the advanced configuration. Both were also very helpful with insights to the design problem.

References

[1]McCullers, L. A., "Aircraft Configuration Optimization Including Optimized Flight Profiles," *Proceedings of Symposium on Recent*

Experiences in Multidisciplinary Analysis and Optimization, edited by J. Sobieski, NASA CP-2327, April 1984, pp. 395–412.

[2]Vanderplaats, G. N., "Automated Optimization Techniques for Aircraft Synthesis," AIAA Paper 76-909, Sept. 1976.

[3]Haftka, R. T., Grossman, B., Eppard, W. M., and Kao, P. J., "Efficient Optimization of Integrated Aerodynamic-Structural Design," *International Journal of Numerical Methods in Engineering*, Vol. 27, 1989, pp. 593–607.

[4]Grossman, B., Haftka, R. T., Kao, P.-J., Polen, D. M., Rais-Rohani, M., and Sobieszczanski-Sobieski, J., "Integrated Aerodynamic-Structural Design of a Transport Wing," *Journal of Aircraft*, Vol. 27, No. 12, 1990, pp. 1050–1056.

[5]Mason, W. H., "Analytic Models for Technology Integration in Aircraft Design," AIAA Paper 90-3262, Sept. 1990.

[6]Wakayama, S., and Kroo, I. M., "A Method for Lifting Surface Design Using Nonlinear Optimization," AIAA Paper 90-3290, Sept. 1990.

[7]Sobieszczanski-Sobieski, J., "Sensitivity Analysis and Multidisciplinary Optimization for Aircraft Design: Recent Advances and Results," *Proceedings of the 16th Congress of the International Council of Aeronautical Sciences*, ICAS-88-1.7.3, Jerusalem, Israel, Aug. 1988, pp. 953–964.

[8]Livne, E., Friedmann, P. P., and Schmit, L. A., "Studies in Integrated Aeroservoelastic Optimization of Actively Controlled Composite Wings," *Proceedings of the AIAA/ASME/ASCE/AHS/ASC 32nd Structures, Structural Dynamics and Materials Conference*, (Baltimore, MD), AIAA, Washington, DC, 1991, pp. 447–461 (AIAA Paper 91-1098).

[9]Unger, E. R., Hutchison, M. G., Rais-Rohani, M., Haftka, R. T., and Grossman, B., "Variable Complexity Multidisciplinary Design of a Transport Wing," *International Journal of Systems Automation Research and Applications (SARA)*, Vol. 2, 1992, pp. 87–113.

[10]Robins, A. W., et al., "A Concept Development of a Mach 3.0 High-Speed Civil Transport," NASA TM 4058, Sept. 1988.

[11]Covell, P., Hernandez, G., Flamm, J., and Rose, O. J., "Supersonic Aerodynamic Characteristics of a Mach 3 High-Speed Civil Transport Configuration," AIAA Paper 90-3210, Sept. 1990.

[12]Craidon, C. B., "Description of a Digital Computer Program for Airplane Configuration Plots," NASA TM X-2074, 1970.

[13]Barnwell, R., "Approximate Method for Calculating Transonic Flow About Lifting Wing-Body Configurations," NASA TR R-452, April 1976, pp. 58–61.

[14]Mason, W. H., Siclari, M. J., Miller, D. S., and Pittman, J. L., "A Supersonic Maneuver Wing Designed for Nonlinear Attached Flow," AIAA Paper 83-0425, Jan. 1983.

[15]Hutchison, M. G., Unger, E. R., Mason, W. H., Grossman, B., and Haftka, R. T., "Variable-Complexity Aerodynamic Optimization of an HSCT Wing Using Structural Wing-Weight Equations," AIAA Paper 92-0212, Jan. 1992.

[16]Coen, P., personal communication, NASA Langley, Hampton, VA, Feb. 1991.

[17]Harris, R. V., Jr., "An Analysis and Correlation of Aircraft Wave Drag," NASA TM X-947, 1964.

[18]Schemensky, R. T., "Development of an Empirically Based Computer Program to Predict the Aerodynamic Characteristics of Aircraft," Vol. 1, Air Force Flight Dynamics Lab. TR-73-144, Dayton, OH, Nov. 1973.

[19]Carlson, H. W., and Miller, D. S., "Numerical Methods for the Design and Analysis of Wings at Supersonic Speeds," NASA TN D-7713, 1974.

[20]Carlson, H. W., Mack, R. J., and Barger, R. L., "Estimation of Attainable Leading-Edge Thrust for Wings at Subsonic and Supersonic Speeds," NASA TP-1500, 1979.

[21]Jones, R. T., and Cohen, D., *High Speed Wing Theory*, Princeton Univ. Press, Princeton, NJ, 1960, pp. 197–202.

[22]Hopkins, E. J., and Inouye, M., "An Evaluation of Theories for Predicting Turbulent Skin Friction and Heat Transfer on Flat Plates at Supersonic and Hypersonic Mach Numbers," *AIAA Journal*, Vol. 9, No. 6, 1971, pp. 993–1003.

[23]Diederich, F. W., "A Planform Parameter for Correlating Certain Aerodynamic Characteristics of Swept Wings," NACA TN-2335, 1951.

[24]Hutchison, M. G., Huang, X., Mason, W. H., Haftka, R. T., and Grossman, B., "Variable-Complexity Aerodynamic-Structural Design of a High-Speed Civil Transport Wing," AIAA Paper 92-4695, Sept. 1992.

[25]Grandhi, R. V., Thareja, R., and Haftka, R. T., "NEWSUMT-A: A General Purpose Program for Constrained Optimization Using Constraint Approximations," *Journal of Mechanisms, Transmissions and Automation in Design*, Vol. 107, 1985, pp. 94–99.

[26]Haftka, R. T., "Combining Global and Local Approximations," *AIAA Journal*, Vol. 29, No. 9, 1991, pp. 1523–1525.